FERMILAB-PROPOSAL-0981

Version 1.4
March 6, 2008

Letter of Intent: Antimatter Gravity Experiment at Fermilab

A. D. Cronin
University of Arizona, Tucson, Arizona 85721, USA

A. P. Mills, Jr.
University of California, Riverside, California 92521, USA

T. J. Phillips*
Duke University, Durham, North Carolina 27708, USA

B. C. Brown, M. Fischler, A. Hahn, J. T. Volk, G. P. Yeh
Fermilab, Batavia, Illinois 60510, USA

J. R. Babcock, S. D. Howe, G. P. Jackson, J. M. Zlotnicki
Hbar Technologies, LLC, West Chicago, Illinois 60185, USA

D. M. Kaplan,* T. J. Roberts[1]
Illinois Institute of Technology, Chicago, Illinois 60616, USA

G. A. Horton-Smith
Kansas State University, Manhattan, Kansas 66506, USA

H. R. Gustafson
University of Michigan, Ann Arbor, Michigan 48109, USA

G. Bonvicini
Wayne State University, Detroit, Michigan 48202, USA

*Contact person; email: Thomas.Phillips@duke.edu.
*Contact person; email: kaplan@iit.edu.

Abstract

Fermilab's unique ability to accumulate large numbers of antiprotons makes it possible to directly measure the gravitational force on antimatter for the first time. Such a measurement will be a fundamental test of gravity in a new regime, directly testing both the equivalence principle and the prediction of General Relativity that matter and antimatter behave identically in the gravitational field of the earth. We propose to decelerate antiprotons in the Main Injector and transfer them into an antihydrogen-production Penning trap. The antihydrogen will emerge from the trap in a low-velocity beam and pass through an atomic interferometer where the gravitational deflection will be measured. A 1% measurement should be possible soon after antihydrogen production is established. A possible follow-on phase of the experiment (beyond the scope of this LoI) can use laser-based interferometry techniques to measure much more precisely any difference between the gravitational forces on matter and antimatter and search sensitively for a possible "fifth force" significantly weaker than gravity.

[1]Also at Muons, Inc.

Contents

1 Motivation **2**

2 Method **3**
2.1 Low-Energy Antimatter 3
2.2 Antihydrogen Production 4
2.3 Measuring $\bar{g}$ with an Interferometer 10
2.4 Antihydrogen Detection 14

3 High Precision Measurement **16**

4 Other Related Efforts **17**
4.1 Comparison with the Present Proposal 18

5 Summary **19**

1 Motivation

Most physicists expect the gravitational acceleration of antimatter to be no different from that of matter, but this belief has not been directly verified by experiment. The theory of General Relativity (GR) is based upon the equivalence principle, which states that the force of gravity on any object is independent of the object's composition. This principle has been verified to high precision with matter, and GR has strong experimental support. Proposed quantum theories of gravity generally include additional terms that can violate the equivalence principle and/or the inverse-square dependence on distance [1]. The direct measurement of the acceleration of antimatter in the Earth's gravitational field is a way to test a fundamental assumption of GR in a new way. Even if the result turns out to be consistent with the predictions of GR it would extend the equivalence principle and be a classic test of that theory, and a possible follow-on, high-precision measurement will be sensitive to possible new forces much weaker than gravity.

To date, experiments have not even ruled out the possibility that antimatter in the gravitational field of the earth will rise rather than fall.[2] Physicists have on occasion argued that K^0 mixing already implies stringent limits on possible differences between the gravitational interactions of matter with matter and of matter with antimatter [2].[3] But it has also been argued that the observed CP violation in the K^0 system may in fact be a consequence of gravitational repulsion between quarks and antiquarks [3, 4]. In the end, the best way to determine the gravitational force on antimatter is a direct

[2] As remote as this possibility may seem, it has been considered in the literature, including speculation that it could provide an alternative explanation for the observed cosmic baryon asymmetry [5]; even a possible role in dark energy has been suggested [4].

[3] See Sec. 4 for discussion of other relevant limits.

measurement. We are proposing to make this measurement at Fermilab in the near future for a modest cost.

2 Method

The gravitational force on antimatter can be measured by directing a low-velocity beam of antihydrogen through an atomic interferometer and measuring the gravitational phase shift [6, 7]. The atomic interferometer can transmit a large fraction of the beam, and the amount by which the interference pattern shifts as the beam traverses the interferometer measures the gravitational deflection of the beam, so it is possible to efficiently measure deflections on the scale of the interference pattern. Details of antihydrogen production and the interferometer are discussed below.

2.1 Low-Energy Antimatter

Antiprotons from Fermilab's antiproton source can be decelerated in the Main Injector and transferred to a new experimental enclosure at MI-9. Such operation has been previously discussed by Jackson [8], and some planning and partial construction for it has already occurred. Plans for the enclosure are shown in Figure 1. Deceleration of protons in the Main Injector has already been demonstrated to 3 GeV/c [9]. Demonstrating that the Main Injector magnets can ramp down to 2 GeV/c was accomplished during the same studies, and an advancement in RF technology developed by Hbar Technologies, LLC now makes deceleration of antiprotons down to 1 GeV/c possible with existing FNAL infrastructure. Studies of deceleration ramps can be done without beam in the Main Injector, and six 4-hour study periods with a proton beam are sufficient to determine whether 1 GeV/c (or lower) is achievable.

A carrier pipe, shown in Figure 2, was already installed for a low-energy transfer line to bring the antiprotons to the new experimental enclosure to be built at MI-9. Here the antiprotons can either be decelerated further in a small ring, or at the cost of some inefficiency, simply run through a degrader to reduce their energy to the point where they can be caught in a Penning trap. Design studies have been performed to estimate the yield of trapped antiprotons using degrader parameters given in Table 1 (see Figure 3). While the design may not be fully optimized, preliminary results indicate an efficiency of $\approx 5 \times 10^{-4}$. Once in a Penning trap, antiprotons are easily cooled to cryogenic temperatures by electrons in the trap. The electrons cool by synchrotron radiation to the temperature of the trap walls, and the antiprotons are cooled by collisions with the electrons [10].

NASA is currently packaging up their High Performance Antiproton Trap (HiPAT) and related equipment, shown in Figures 4 and 5, for shipping to HBar Technologies. This trap will be used for the gravity measurement. The existing HiPAT cryostat is already configured to meet the needs of the experiment. The H^- and proton sources and associated optics are also already configured to commission the experiment. Some

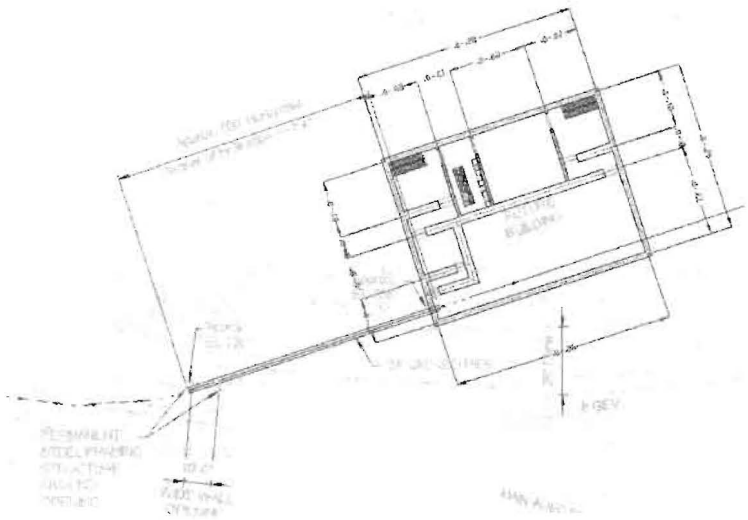

Figure 1: Design for an experimental enclosure to be built at MI-9 to house experiments using low-energy and trapped antiprotons.

modification to the existing electrode structure is needed for the initial commissioning of the experiment, and we anticipate that a new electrode structure optimized for low-velocity antihydrogen formation will be built. The new structure will be housed in a vacuum pipe with ends that mate to gate valves and include non-intercepting vacuum connections that allow antiproton injection from one end and antihydrogen emission from the other end.

To make antihydrogen, positrons are needed in addition to antiprotons. Positrons with the needed parameters can be accumulated from a ^{22}Na source using apparatus that is now commercially available [11]. This source, shown in Figure 6, can provide 8×10^6 positrons/sec from a 50 mCi ^{22}Na source. The positrons are accumulated in a trap using a differentially pumped spoiled vacuum [12]. The ATHENA collaboration has used this technique to achieve positron densities of $2.6 \times 10^{10}/\text{cm}^3$ [13].

2.2 Antihydrogen Production

Two groups at CERN have been making antihydrogen at the CERN Antiproton Decelerator (AD) since 2002 [14, 15]. The primary goal of these groups has been to trap antihydrogen in order to perform spectroscopy for high-precision *CPT* tests, so they are attempting to produce antihydrogen with extremely low velocity. Antihydrogen is produced by trapping cold antiprotons and positrons in separate potential wells in a Penning trap and causing the antiprotons to overlap with the positron plasma.

The velocity distribution of the antihydrogen produced by the ATRAP collaboration is shown in Figure 7. The antihydrogen is made in a beam along the axis of the trap

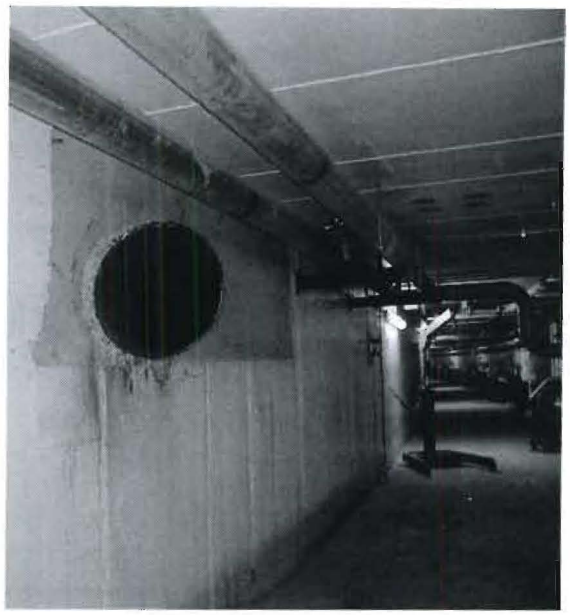

Figure 2: End of carrier pipe where it penetrates the wall of the Main Injector tunnel. This pipe was installed to enclose a low-energy beamline from the Main Injector at MI-10 to the experimental hall at MI-9. The four penetrations on the ceiling also lead to the location of the future MI-9 enclosure.

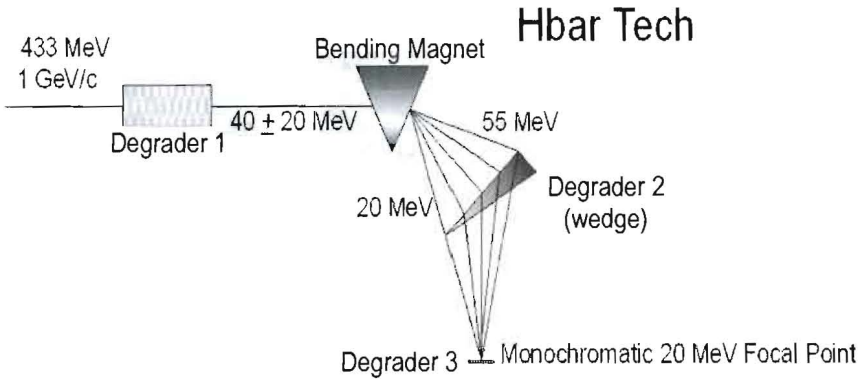

Figure 3: Degrader design studied by Hbar Technologies, LLC.

Table 1: Degrader configuration studied.

Intial $\bar{p}$ momentum:		$1\,\mathrm{GeV}/c$
Degrader 1:	geometry	cylindrical
	material	Fe
	thickness	16.75 cm
	$\bar{p}$ survival	50%
Degrader 2:	geometry	magnetic wedge
	$\bar{p}$ survival	~100%
Degrader 3:	geometry	foil
	material	Al
	thickness	$25\,\mu$m
	$\bar{p}$ survival	50%
Trap injection efficiency:		0.2%
Overall efficiency:		5×10^{-4}

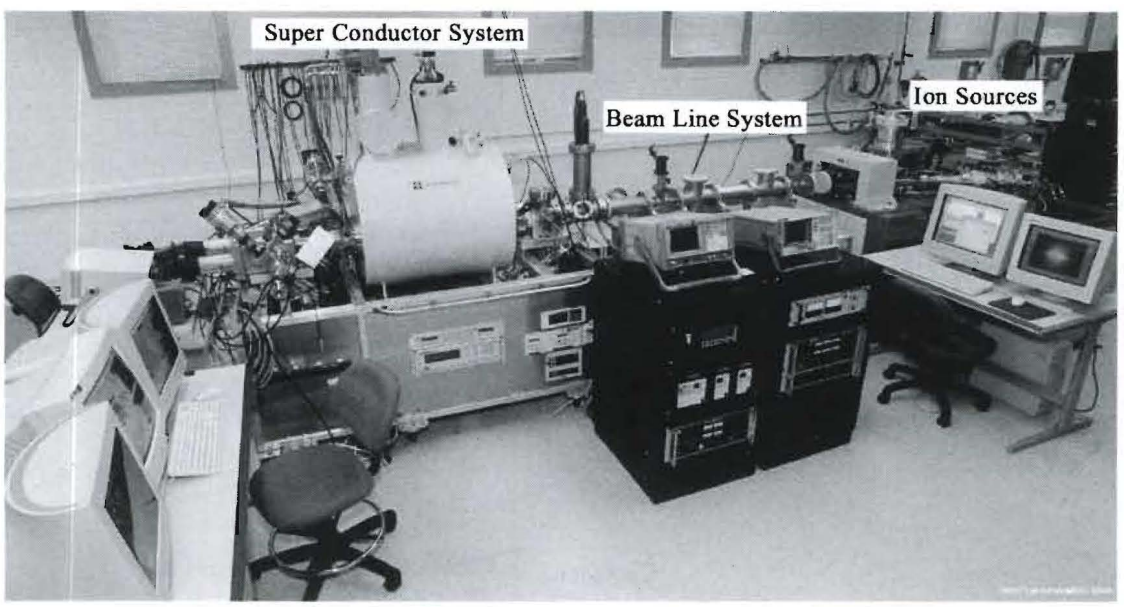

Figure 4: NASA's High Performance Antiproton Trap (HiPAT), which will be used for the Antimatter Gravity Experiment.

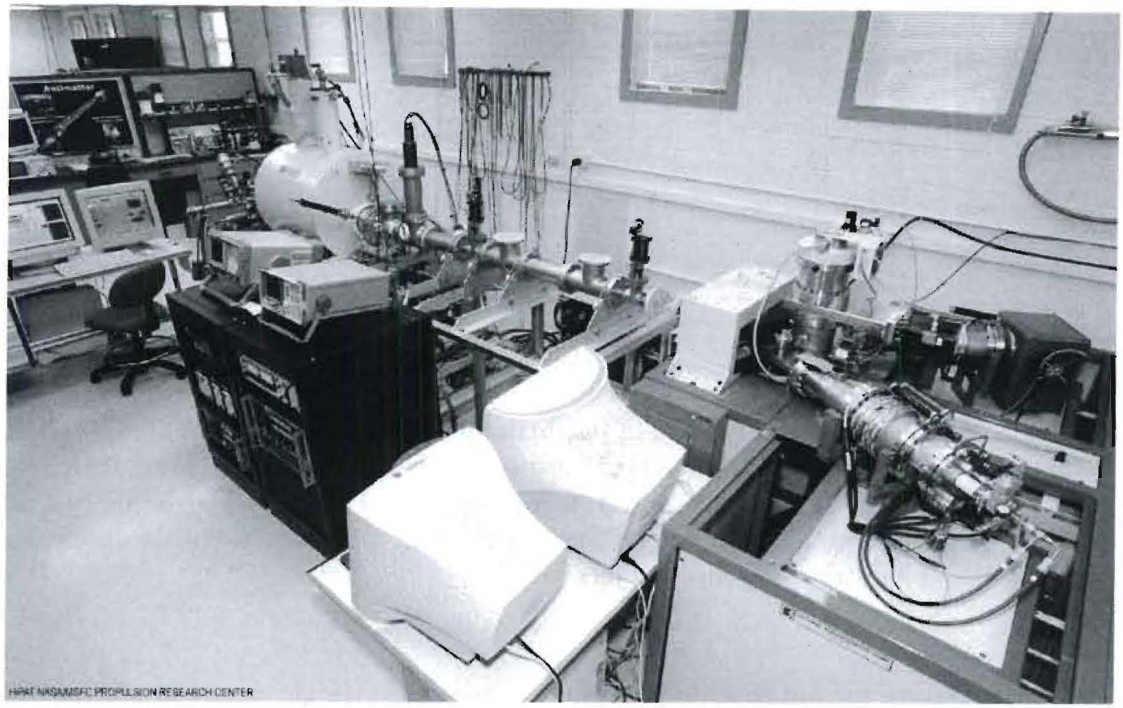

Figure 5: Ion sources for HiPAT.

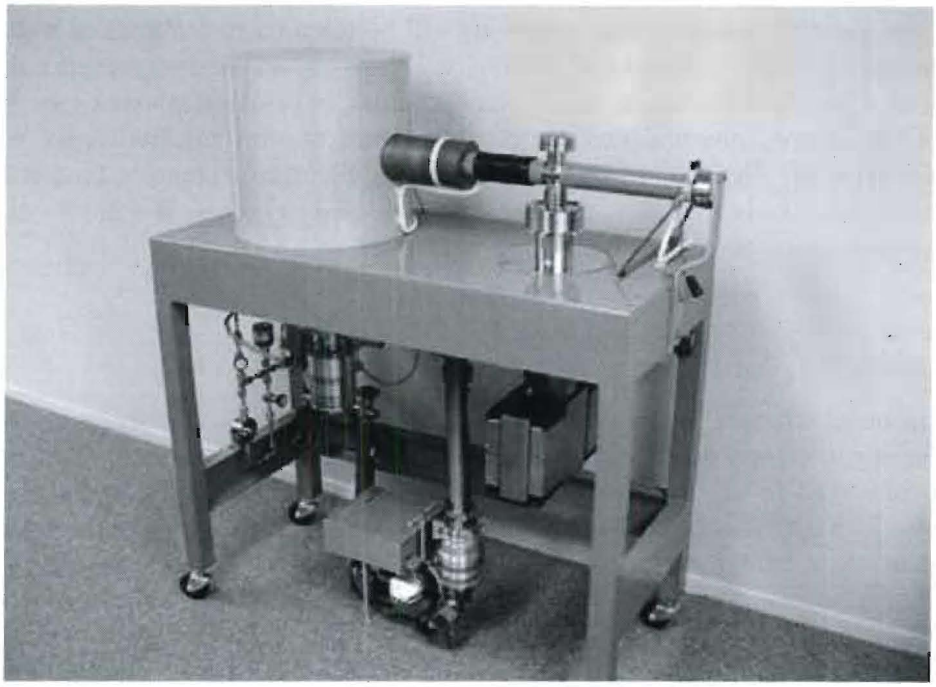

Figure 6: A commercially available positron source [11].

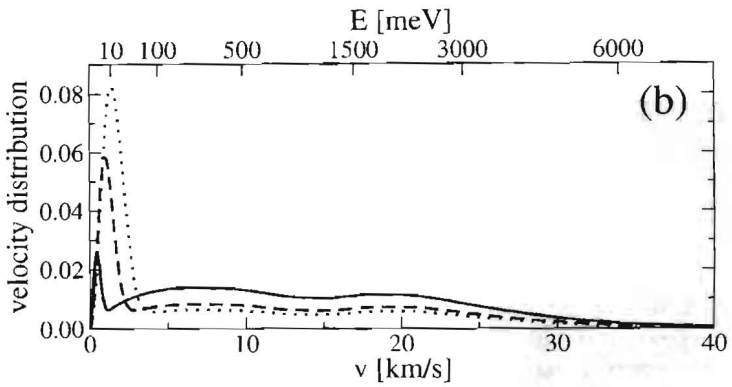

Figure 7: The velocity distribution of antihydrogen produced by the ATRAP collaboration. The three curves are for average antiproton velocities corresponding to $K_B T_{\bar{p}} =$ 1 meV (solid), 2 meV (dashed), and 5 meV (dotted). The long, high-velocity tail is believed to come from antihydrogen atoms that charge-exchange with hot antiprotons in side wells of the trap. (From reference [16].)

by gently heating the antiprotons so that they pass through the positron plasma. The low-velocity peak corresponds to the energy given the antiprotons, while the long, high-velocity tail is believed to come from charge exchange of these low-velocity antihydrogen atoms with hot antiprotons in side wells of the trap [16].

For the gravity measurement, positrons will be trapped in a potential well separate from the antiprotons, and the antiprotons will be accelerated by a small voltage to a velocity of a few km/sec before they pass through the positron plasma (see Figure 8). Some of the antiprotons will pick up positrons and become antihydrogen, which will exit the trap in the direction of the antiproton's momentum. The rate for antihydrogen production in a strong magnetic field by the three-body reaction $\bar{p} + 2e^+ \rightarrow \overline{\mathrm{H}} + e^+$ has been calculated [17] to be

$$\Gamma = 6 \times 10^{-13} \left(\frac{4.2}{T}\right)^{9/2} n_e^2 \, [\mathrm{s}^{-1}] \tag{1}$$

per antiproton, where T is the absolute temperature and n_e is the positron density per cm^3. For a sufficiently high positron density, a significant fraction of the antiprotons will be converted to antihydrogen every time they pass through the positron plasma. For example, with conservative values of $n_e > 10^7/\mathrm{cm}^3$ at a temperature of 4.2 K, each antiproton has a >0.6% chance of becoming an antihydrogen when passing through a 10-cm-long positron plasma at 1 km/s. This may be an underestimate; for example, this calculation neglects radiative combination and the three-body reaction $2\bar{p} + e^+ \rightarrow \overline{\mathrm{H}} + \bar{p}$, which should enhance the antihydrogen production rate for the high antiproton densities achievable at Fermilab. However, we show below that there is a substantial margin for the measurement even if the production rate is substantially below this

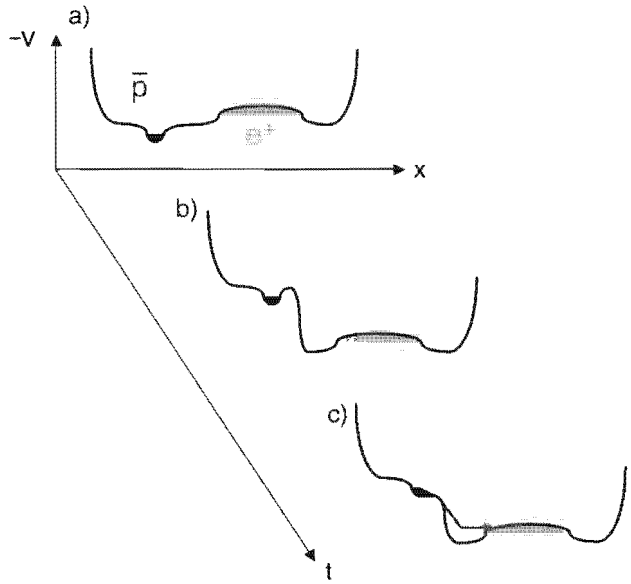

Figure 8: Cartoon of a) trap potential vs x at $t = 0$ showing antiprotons (red) and positrons (green) in separate wells (note that due to their opposite charges they are portrayed as sitting "above" and "under" their wells, respectively); b) and c) are snapshots showing voltage manipulations to accelerate the antiprotons such that they pass through the positrons: at time b), the $\bar{p}$ well potential is "raised" (made more negative) in preparation for $\bar{p}$ acceleration; at time c), the potential barrier between the $\bar{p}$ and e^+ wells is dropped and the $\bar{p}$'s are accelerated through the e^+ well.

estimate.

Since the gravitational deflection measured by the interferometer is a function of velocity, either the $\overline{\mathrm{H}}$ beam needs to have a narrow, well-defined velocity distribution, or the velocity of individual antihydrogen atoms needs to be measured. By accelerating the antiprotons through the positron plasma with a known voltage at a specified time, not only will the velocity be known to within the thermal velocity spread of the antihydrogen, but we can also measure the velocity by recording the time of flight.

Antiprotons that do not make antihydrogen will remain in the trap and be recycled. There are a number of ways of handling this. For example, voltages can be applied that keep the antiprotons synchronized as they oscillate back and forth through the positrons. In any case it is likely that half of the antihydrogen atoms would be produced going in the wrong direction, but it should be possible to recapture most of these by field ionizing the antihydrogen that goes in the wrong direction.

Because most of the antiprotons that are not converted into antihydrogen on a single pass through the positron plasma can be recycled, the efficiency for making antihydrogen on a single pass is not a critical parameter. It will only affect the total number of cycles needed to convert the antiprotons to antihydrogen. The cycle time is likely to be

of order 10 ms; using this assumption and a 0.6% probability for creating antihydrogen per antiproton per cycle, then the time needed to convert half the antiprotons into antihydrogen is just over a second. The time to convert half the antiprotons to antihydrogen is still under two hours for a conversion probability of one in a million. To minimize impact on integrated Tevatron luminosity, and because a small fraction of the Antiproton Source production rate suffices for the proposed measurement, transfers of antiprotons are expected to be infrequent. Thus there is plenty of margin for the additional cycles that would be required should the antiproton-to-antihydrogen conversion probability turn out to be lower than estimated here.

As noted above, the high antiproton densities achievable at Fermilab will allow for an antihydrogen production mechanism that, to our knowledge, has not been considered for antihydrogen production at CERN. At the AD, it is expected that a dominant antihydrogen production mechanism is the three-body reaction $\overline{p}+2e^+ \rightarrow \overline{\mathrm{H}}+e^+$, which leaves most of the antihydrogen in a (highly excited) Rydberg state [18]. However, with a sufficiently high antiproton density the three-body reaction $2\overline{p} + e^+ \rightarrow \overline{\mathrm{H}} + \overline{p}$ should become important, and this charge-exchange reaction leaves the antihydrogen more tightly bound [16]. The charge-exchange reaction has been serendipitously observed at CERN with hot antiprotons in side wells [16]. We propose to take advantage of this reaction by tailoring the release of antiprotons such that faster antiprotons would overtake slower antiprotons as they pass through the positron plasma. At this time we do not have a calculated rate for this reaction, but we expect it to be substantial because of the large fraction of antihydrogen that experienced charge exchange in the ATRAP experiment [16].

The antihydrogen production mechanism has been studied by the ATHENA Collaboration [19]. While the observed temperature dependence does not match the expectation for the three-body reaction $\overline{p} + 2e^+ \rightarrow \overline{\mathrm{H}} + e^+$, the rate is at least an order of magnitude higher than expected from radiative combination. So while the mechanisms for making antihydrogen are still not completely understood, it is clear that it is possible to make antihydrogen at a significant rate and with a velocity distribution appropriate for the gravity measurement.

2.3 Measuring $\bar{g}$ with an Interferometer

The most obvious method to measure $\bar{g}$ using the antihydrogen beam would be to collimate the beam horizontally and measure its position after it had propagated a sufficient distance in a drift tube. However, this method makes inefficient use of the antihydrogen. A more efficient measurement can be made using an interferometer. The concept is to set up an interference pattern with a pair of diffraction gratings, and to measure the phase of the interference pattern with a third grating. The phase shift caused by gravitation can be measured by comparing the phase shifts for beams of different velocities. The axis of the interferometer can also be rotated with respect to the direction of gravity; when the grating lines are vertical gravity will not affect the interference pattern. Calibrations with matter beams are possible as well.

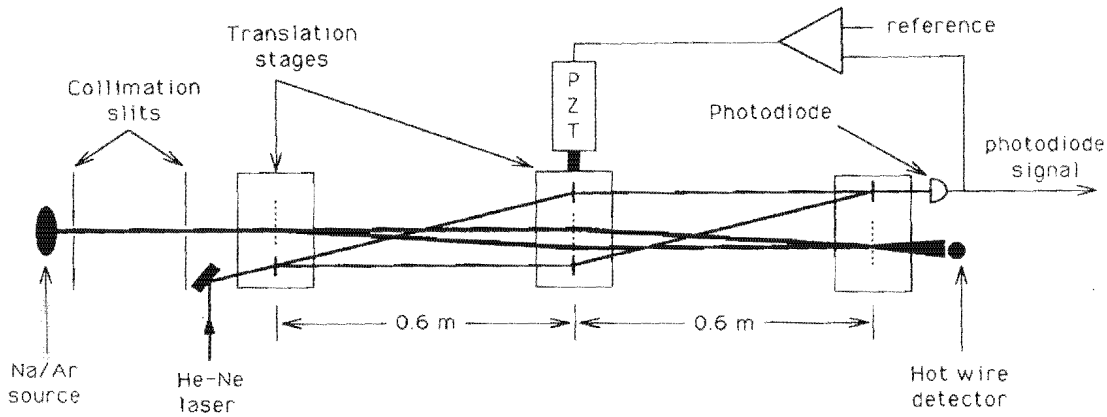

Figure 9: Schematic of the sodium-atom interferometer in use at MIT. A similar interferometer can be used with antihydrogen to measure the gravitational force on antimatter. Separated beams are not needed for the gravity measurement, so the collimator is unnecessary and the period of the diffraction gratings can be much larger. (From reference [20].)

Perhaps the ideal interferometer for this experiment is a configuration that has been used for both neutron and atom interferometry [20,21] (Figure 9). This interferometer consists of three equally spaced transmission gratings, each with identical line spacing. The first two gratings set up an interference pattern that is independent of both wavelength and the spatial coherence (incident wave direction) of the source [22]. This interference pattern has a spatial period equal to the line spacing of the gratings, so the phase of the interference pattern can be analyzed by using a third identical grating as a mask and measuring the transmission as a function of the mask's position. The interference pattern is localized in x (the direction perpendicular to the grating planes), so while the distance between the first and second gratings is arbitrary, the distance from the second to the third grating must match the distance between the first and second gratings. A diagram illustrating the principle of the interferometer is shown in Figure 10 and an example interference pattern is shown in Figure 11.

Not all of the diffraction orders from the first two gratings will contribute to the interference pattern. However, by using gratings with roughly 50% transmission (i.e., the slit width is half of the grating period), the even diffraction orders are suppressed, and most of the transmitted beam appears in the 0th and $\pm 1^{st}$ orders in roughly equal amounts. The orders that will interfere are shown in Figure 10. Ideally, approximately 4/9 of the beam transmitted through the second grating (four of the nine principle diffraction orders) will contribute to the interference pattern.

The phase of the interference pattern can be measured by moving the third grating in the $\hat{y}$ direction. The transmission is then recorded as a function of the phase of the grating: the transmission is highest when the interference peaks fall on the slits.

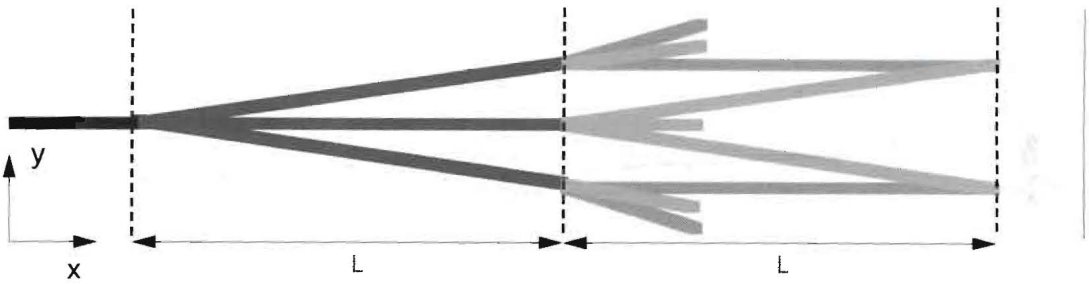

Figure 10: Principle of three-grating interferometer for measuring $\bar{g}$. The three diffraction orders shown will contain most of the transmitted beam in roughly equal amounts. The orders that are drawn to the third grating cause an interference pattern with a frequency that matches the grating's line spacing. The diffraction orders that are not followed to the third grating do not contribute to this pattern, but rather cause a flat background.

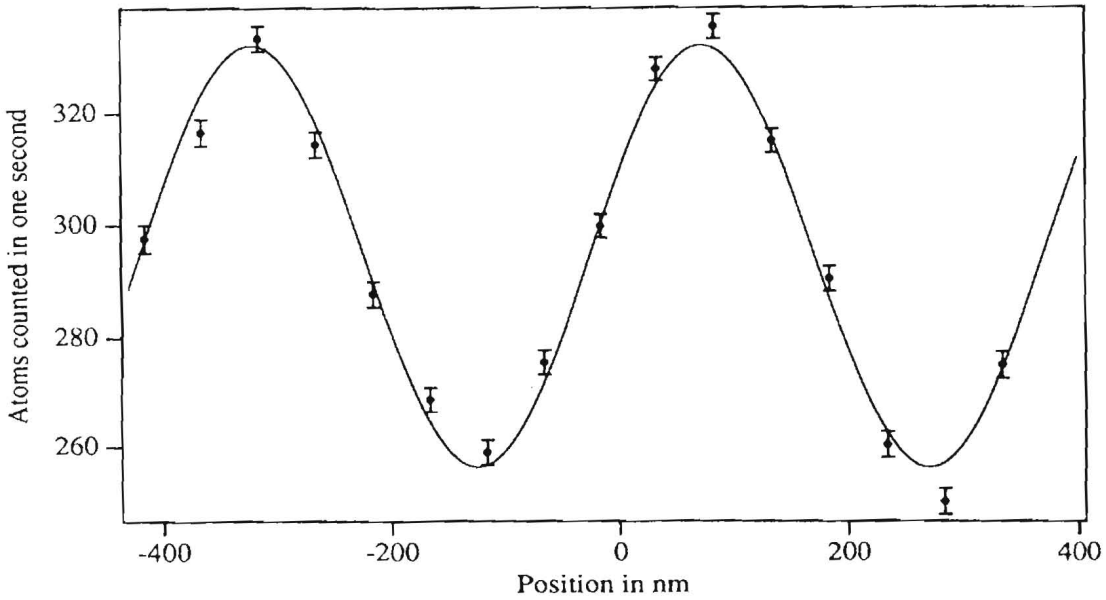

Figure 11: Interference pattern measured using sodium atoms in the MIT interferometer from 400 seconds of data; note suppressed zero. (From reference [20].)

The interference pattern shifts by the same amount that transmitted atoms are deflected while transversing the interferometer. Thus, for deflection D given by

$$D = \bar{g}\frac{L^2}{v^2}\,, \tag{2}$$

where L is the separation between successive gratings and v is the velocity of the antihydrogen, the resulting phase shift $\Delta\phi$ is

$$\Delta\phi = 2\pi D/d\,, \tag{3}$$

where d is the line spacing of the grating. It is important to note that while the interference pattern is independent of velocity (wavelength), the deflection (or equivalently the phase shift) due to gravity is not. This means that a large velocity dispersion can wash out the interference pattern when the phase shift due to gravity becomes significant, so the beam used to make this measurement must either have a sufficiently small velocity dispersion, or else the velocity of each antihydrogen atom must be measured.

We can illustrate this method for measuring the force of gravity using the parameters for a prototype interferometer that is under construction for this project by T. Phillips, working with a beam of metastable hydrogen atoms (rather than the currently unavailable antihydrogen). (The metastable beam provides a clean signature relative to background hydrogen in the apparatus.) This interferometer has gratings with $d = 1\,\mu$m and $L = 62$ cm. A beam of hydrogen traveling at 3 km/s would experience a gravitational deflection of $0.4\,\mu$m which corresponds to a phase shift of 0.8π rad for the interference pattern. The limiting uncertainties in calculating g from this measurement are likely to come from uncertainty in the velocity of the hydrogen atoms and uncertainty in the grating position. If we assume the hydrogen atoms are excited to the metastable state over a 1 cm region and the distance to the detector is 250 cm, then the uncertainty in the velocity measurement will be 0.4%. In order to match this uncertainty, the phase shift would need to be measured to 5 mrad. Reducing the beam velocity to 1 km/s would increase the deflection to $3.8\,\mu$m (7.5π rad) and the phase shift would need to be known to 48 mrad.

By using the interferometer used with sodium atoms [20] as an example, we estimate that we should be able to make a 1% measurement of $\bar{g}$ with a few $\times\, 10^5$ antihydrogen atoms incident upon the first grating of the interferometer. If the order of magnitude of the antihydrogen production rate calculated above is correct, then we should be able to produce many more antihydrogen atoms than this, and the measurement would not be limited by statistics. We expect the leading systematic uncertainty to be how well the dimensions of the interferometer can be controlled and measured.

The antihydrogen velocity distribution shown in Figure 7 would work for the gravity measurement, where the low-velocity peak would experience significant gravitational deflection while the high-velocity tail can be used to monitor the alignment of the interferometer.

The efficiency for the antihydrogen to contribute to the interference pattern will depend upon a number of design parameters, and this can be illustrated by working

through an example. Each grating will have 50% open area, less whatever support structure is needed to keep the grating lines in place. If we take the support structure to be 5% of the area, the net beam transmitted through the first two gratings will be about 23% and on average about 11% will be transmitted through the third grating (the mask). Only four of the nine dominant diffraction orders will contribute to the interference pattern (see Figure 10). Imperfections in the gratings and misalignments will reduce the contrast of the interference pattern so if we take this reduction to be roughly a factor of two then about 3% of the beam will contribute to the interference pattern. Transmitted antihydrogen atoms annihilate on a final screen located a suitable distance downstream of the third grating, with the annihilation products detected as discussed in the next section. (Note that if desired, we can improve the statistical significance of our signal by separately measuring annihilations that occur on the third grating, in addition to those that occur in the screen.)

A significant inefficiency can arise from the transverse thermal velocity of the antiprotons, which leads to a broadening of the beam. For example, for antiprotons at 4.2 K accelerated with 30 mV to a velocity of 2.4 km/s, the beam would have a half-width of 25 cm at a distance of 225 cm, a reasonable distance for the third grating. It is not practical to have gratings this large; the prototype gratings mentioned above are about 1 cm in diameter, so would accept only 0.03% of the beam. This can be approximately quadrupled by lowering the temperature of the antiprotons to 1 K, or it can be raised to 2.1% by using 4-inch gratings [23], in which case lowering the antiproton temperature to 1 K again approximately quadruples the efficiency to 8.6%. Of course, the cost of lowering the antiproton temperature will need to be considered along with other technical considerations in determining the optimal configuration. Another way to raise the efficiency for converting antiprotons into antihydrogen that traverses the interferometer is to collimate by field-ionizing antihydrogen that would miss the interferometer, and then return the stripped antiprotons to the production trap.

These considerations are summarized in Table 2, based on representative performance assumptions discussed above. While it is premature to give precise estimates, and some of the efficiencies in Table 2 may well increase as the design is refined, at the order-of-magnitude level this estimate indicates the great potential of such an experiment at Fermilab. (For example, it far exceeds the intensities available at the CERN Antiproton Decelerator.) To the extent possible, we intend to refine these estimates over the next several months, although we recognize that some of them may require tests with trapped $\bar{p}$'s to establish with confidence.

2.4 Antihydrogen Detection

Antihydrogen annihilation in matter produces large signals which are easily detected in scintillator, silicon detectors, and wire chambers. It is possible to conduct this experiment by simply counting the net transmission through the interferometer with scintillators, but additional information gathered with more sophisticated detectors can add statistical power and aid in controlling systematic uncertainties. If possible,

Table 2: Illustrative rate estimates for antihydrogen production and detection (assuming 4″ gratings, 4.2 K operation, and use of a field-ionizing collimator).

$\bar{p}$ pulses/day	1
$\bar{p}$'s/pulse	10^{10}
Trapping efficiency	5×10^{-4}
Trapped $\bar{p}$'s/pulse	5×10^{6}
$\overline{\mathrm{H}}$ formation efficiency	10%
$\overline{\mathrm{H}}$'s/pulse incident on 1st grating	5×10^{5}
Background (noninterfering) $\overline{\mathrm{H}}$'s/pulse	5×10^{4}
$\overline{\mathrm{H}}$'s in interference pattern/pulse	10^{4}

the antihydrogen detector should monitor annihilation rates at each grating and at the final screen, which are separated by a few meters. Because the velocity measurement is crucial to our experiment, time resolution well below 1 ms is a necessity. Spatial resolution in the direction transverse to the beam should be as fine as possible, so that (ideally) the interference fringe pattern on the third grating and the final screen can be seen in as much detail as possible to aid in aligning the interferometer.

While there are many options that could be considered, a simple, economical, and trouble-free way of achieving these goals is by using one of the recently decommissioned large drift chambers from either CLEO or BABAR. Besides being complete (all hardware components plus online and offline software) and high-precision systems, as well as tolerant of fairly high rates, these drift chambers are long enough that the whole setup can be monitored with a single device. These devices are also self-triggering, which means that there is no need for additional detectors.

The BABAR drift chamber is 276 cm in length. The relevant parameters of the CLEO-c drift chamber are summarized in Table 3 (the spatial resolutions are taken directly from the CLEO Caliper web pages). When operated in their original environment, these detectors provide a measurement of five quantities per track: three momentum components and two distances of closest approach to the origin.

In the Antimatter Gravity experiment, there is no equivalent of the "Beam" signal, which provides the t_0 to the whole CLEO or BABAR detector. The chamber data are fitted in such a way as to extract two angles, two distances and one time for each track. Annihilation events with two or more charged tracks can be used to reconstruct precisely the location of the annihilation vertex and its most probable time. This technique is used routinely in CLEO to measure the size and shape of the luminous region at the interaction point, and most notably to monitor the bunch length, a quantity of great interest to the machine operators.

Assuming that the chambers can be transported and restarted without damage to their components or large misalignments, one expects a similar performance as in CLEO or BABAR. On one hand, due to the absence of a magnetic field, one has

Table 3: Summary of CLEO-c Drift Chamber nominal parameters, as applicable to the Antimatter Gravity experiment.

Parameter	Unit	Value
Wire length	cm	73–237
Inner diameter	cm	35
σ_x	μm	40–50
σ_z	μm	200
σ_t	ns	<50

a better-known time-to-distance relation in the drift cells, smaller overall correlation coefficients among the tracking parameters, and lesser multiple scattering between interaction point and tracker. On the other hand, without an inner detector, overall spatial resolution will be degraded by perhaps a factor of two.

From Table 3 one can see that the estimated timing resolution is excellent (below 50 ns) and probably exceeds the precision with which one knows the time of production of the antihydrogen. By reconstructing annihilation vertices on the third grating and on the final screen we will be able to observe characteristic interference fringes if the interferometer is rotationally misaligned. We will also be able to use the resolution along the beam direction (called σ_z in Table 3) to reconstruct the position of the gratings.

The use of a tracking detector to observe antihydrogen annihilations will provide far more detailed information about the annihilations than scintillators would, but it will also add considerable complexity to the experiment. We have not yet sought permission to use either of these drift chambers, and we will need to carefully weigh the benefits against the additional costs before determining the best way to detect antihydrogen annihilations.

3 High Precision Measurement

Should the initial measurement prove unable to distinguish the gravitational force on antimatter from that on matter, it would be desirable to make a precision measurement of the difference between the gravitational forces on matter and antimatter. This would be sensitive, for example, to a weak fifth force that coupled to baryon number. Atomic interferometers have been used to measure the gravitational force on matter to a part in 10^{10} [24]. This is done by launching atoms in an atomic fountain and using a laser pulse to split the atoms into a superposition of momentum states. These states separate in space, and a second laser pulse brings the states back together where they are recombined with a third laser pulse, but with a phase shift that depends upon local g (see Figure 12).

This technique can be used with hydrogen and antihydrogen to make a precision

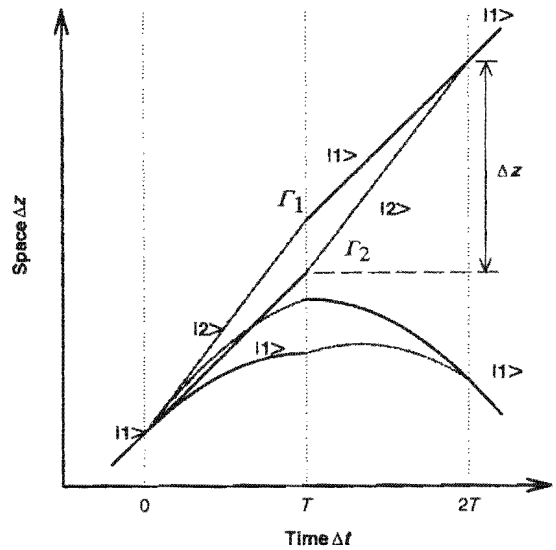

Figure 12: Phase space diagrams, in the presence and absence of gravity, for atom interferometer based upon $\frac{1}{2}\pi - \pi - \frac{1}{2}\pi$ pulse sequence. The first laser pulse splits the atoms into superpositions of two momentum states which separate spatially. The second pulse brings these split states back together, and the third pulse recombines them with a phase shift that depends upon local g. (From reference [24].)

difference measurement of the force of gravity on matter and antimatter [25,26]. However, unlike the initial measurement of $\bar{g}$, this will require a long program to develop the technology needed to trap and cool the neutral antihydrogen atoms.

4 Other Related Efforts

As emphasized in [1], the search for suppressed "non-Newtonian" components of the gravitational force has been an ongoing area of interest despite the difficulty of the experiments. (A review of some of the difficulties encountered may be found in [27].) A number of pioneering searches have nonetheless been carried out over many years. The key measurement using antihydrogen has only recently become feasible and is now proposed at CERN as well as at Fermilab. As we will argue, features of the Fermilab Antiproton Source and its recently developed mode of operation ("stashing" of antiprotons in the Recycler) offer significant advantages at Fermilab vis à vis the CERN AD.

The modern phase of this field can be said to have started with the work of Witteborn and Fairbank [28]. Although, due to Fairbank's death in 1989, their plan to make gravitational measurements with positrons did not come to fruition, they did set a limit on anomalous gravitational interactons of electrons. Such measurements using charged (anti)particles are bedeviled by many subtleties of residual electromagnetic

interactions [27]. Despite this, a proposal to measure the gravitational force on a beam of antiprotons was pursued for several years [29], although it ultimately did not lead to a measurement.

A limit on the possible difference between the gravitational interactions of neutrinos and antineutrinos was derived by LoSecco from observations of neutrinos from SN1987a [30]. Nieto and Goldman [1] observe that this observation does not constrain possible deviations from Newtonian gravity on distance scales very much smaller than the size of our galaxy; it also does not necessarily constrain the gravitational interactions of (anti)baryonic matter. (There is also some unavoidable uncertainty whether in fact both neutrino and antineutrino events were detected [31].)

The idea to measure the gravitational acceleration of neutral antimatter (and thereby evade the confounding effects of stray electrical and magnetic fields) has been receiving increasing attention [6, 7, 32–37], as well as considerable recent impetus from the success in forming antihydrogen in traps at the CERN AD. Compared to the ongoing effort to search for *CPT* violation by precisely comparing the atomic spectrum of antihydrogen with that of hydrogen, it does not require the production and trapping of ground-state antihydrogen (a challenging goal that still has not been attained).

Prior to the present proposal, the most recent (both focused on the CERN AD) are that of the AEGIS Collaboration [36] and a competing one [37] involving members of the ASACUSA Collaboration. The AEGIS Collaboration propose a 1% measurement of the gravitational acceleration of antihydrogen atoms using a classical Moiré deflectometer. They discuss a more elaborate scheme than ours, apparently to compensate for the much lower antiproton intensity at the AD. Antihydrogen is to be formed at rest in a Rydberg state in a Malmberg–Penning trap using a charge-exchange reaction with positronium. The desired states of positronium and antihydrogen are to be produced and cooled with the aid of various laser manipulations. They will then accelerate the Rydberg antihydrogen atoms towards the deflectometer via their atomic dipole moments using a gradient electric field (Stark acceleration). The competing Letter of Intent [37] is also under consideration at CERN [38]. It discusses an approach that promises better systematics but lower statistics than that of AEGIS, and projects a 5-year effort culminating in the gravity measurement. The LoI is focused on methods to form $\overline{\mathrm{H}}$ at very low energy by making use of $\overline{\mathrm{H}}^+$ ions. The gravity measurement is described in [35] and involves cooling the antihydrogen to the 100 μK range, dropping it, and measuring the time of flight. The authors expect that this method can determine $\bar{g}$ with a precision better than 0.1%.

4.1 Comparison with the Present Proposal

The feasibility of the present proposal stems from the recent implementation (for the Tevatron Collider) of antiproton "stashing" (with electron cooling) in the Recycler. As a result of this advance, the Recycler at most times during Tevatron operation contains of the order of 10^{12} antiprotons—a number which of course increases as antiproton accumulation progresses, until the stash is transferred to the Main Injector,

accelerated to 120 GeV, and then transferred to the Tevatron for acceleration to 1 TeV and collisions with the counter-rotating 1 TeV proton beam. Apparatus is thus in place, and routinely functioning, that can transfer antiproton bunches from the Recycler to the Main Injector. Not only can the entire stash be transferred from the Recycler to the Main Injector, but it is also feasible to transfer individual bunches one at a time.

Once an antiproton bunch (of typically 10^{10} antiprotons) is transferred to the Main Injector, it can be quickly decelerated using techniques that were developed for this purpose by G. Jackson some years ago during a brief, dedicated study period [9]. The decelerated bunch can then be extracted "up" the Main Injector proton injection line. A needed switching magnet (to prevent the decelerated antiproton bunch from proceeding back into the Booster, and instead divert it to a new MI-9 transfer line to be built) has been designed for this purpose and assembled by Hbar Technologies, LLC [39]. Starting from this decelerated antiproton bunch, as discussed above, even a rather inefficient antihydrogen production mechanism should be capable of yielding of order 10^5 or so antihydrogen atoms (see Table 2), and we expect the rate to be substantially greater than this. By contrast, the AEGIS Collaboration discusses producing ~ 100 to 1000 antihydrogen atoms over the course of some hundreds of seconds. To accomplish this they anticipate accumulating antiprotons in the trap over many AD cycles. As they emphasize, to measure each antihydrogen atom in the AEGIS deflectometer one by one and then combine these for a 1% measurement will require careful attention to alignment stability, monitoring, and calibration over periods of several weeks. (Although it may well be feasible, all in all this does appear something of a technical tour de force, which perhaps provides another rationale for the ASACUSA-inspired LoI [37].)

It should be noted that the impact on both Tevatron luminosity and NuMI integrated flux will be extremely minimal in the operating mode we propose, as only a single bunch of antiprotons need be decelerated, of order once per day, for this effort. The cost of the proposed effort is also anticipated to be small, with advantage taken of many existing resources, and only a handful of newly constructed items required.

5 Summary

A key pillar of our understanding of the universe, General Relativity, has never been directly tested with antimatter. The opportunity to do so lies within our grasp. The results will be of great interest regardless of the outcome. Even the generally expected result will represent a unique and important measurement; a high-precision follow-on phase might then tell us about new forces not yet seen elsewhere. Because most of the needed components already exist, the measurement can be done quickly and inexpensively. This high-profile project will garner enormous positive attention among the general public. It is just and fitting that such an initiative occur at Fermilab, the world's leading antiproton facility. We must act now before the initiative is seized elsewhere.

References

[1] M. M. Nieto and T. Goldman, Phys. Rep. **205** (1991) 221–281.

[2] See e.g. M. L. Good, Phys. Rev. **121** (1961) 311.

[3] G. Chardin and J. Rax, Phys. Lett. B **282** (1992) 256.

[4] G. Chardin, AIP Conference Proceedings **643** (2002) 385.

[5] This mechanism was considered by P. Morrison [Am. J. Phys. **26** (1958) 358], as well as others, before *CP* violation was discovered and suggested by Sakharov as the likely solution to the baryon asymmetry problem; see also R. W. Brown and F. W. Stecker, Phys. Rev. Lett. **43** (1979) 315, who consider it in the context of Grand Unified Theories.

[6] T. J. Phillips, Hyp. Int. **109** (1997) 357.

[7] T. J. Phillips, Proc. $\overline{p}$2000 Workshop, ed. D. M. Kaplan and H. A. Rubin, Illinois Institute of Technology, Chicago, IL, Aug. 3–5, 2000, p. 109 (available from `http://www.capp.iit.edu/~capp/workshops/pbar2000/pbar2000_program.html`)

[8] G. P. Jackson, Proc. 8th European Particle Accelerator Conference (EPAC 2002), Paris, France, 3–7 June 2002, p. 119.

[9] G. P. Jackson, Proc. 2001 Particle Accelerator Conference (PAC01), ed. P. Lucas, S. Webber (IEEE, Piscataway, NJ, 2001), p. 2554.

[10] G. Gabrielse, X. Fei, L. A. Orozco, R. L. Tjoelker, J. Haas, H. Kalinowsky, T. A. Trainor, and W. Kells, Phys. Rev. Lett. **63** (1989) 1360.

[11] See `http://www.firstpsi.com`

[12] R. Greaves, M. Tinkle, and C. Surko, Phys. Plasmas **1** (1994) 1439.

[13] L. Jorgensen et al., Phys. Rev. Lett. **95** (2005) 025002.

[14] M. Amoretti *et al.*, Nature (London) **419** (2002) 456.

[15] G. Gabrielse *et al.*, Phys. Rev. Lett. **89** (2002) 213401.

[16] T. Pohl, H. R. Sadeghpour, and G. Gabrielse, Phys. Rev. Lett. **97** (2006) 143401.

[17] Michael E. Glinsky and Thomas M. O'Neil, Phys. Fluids B **3** (1991) 1279.

[18] F. Robicheaux, Phys. Rev. A **73** (2006) 033401.

[19] M. Amoretti, Phys. Lett. B **583** (2004) 59.

[20] D. W. Keith, C. R. Ekstrom, Q. A. Turchette, and D. E. Pritchard, Phys. Rev. Lett. **66** (1991) 2693.

[21] Manfred Gruber *et al.*, Phys. Lett. A **140** (1989) 363.

[22] B. J. Chang, R. Alferness, E. N. Leith, Appl. Optics **14** (1975) 1592. Alternative interferometers that do not require plane waves are described in J. F. Clauser, M. Reinsch, Appl. Phys. B **54** (1992) 380.

[23] A number of years ago, the SNL laboratory at MIT (`http://snl.mit.edu/`) claimed to be able to fabricate the required 4-inch gratings for a reasonable price. It is likely that their capability has improved since that time.

[24] A. Peters, K. Chung, B. Young, J. Hensley, and S. Chu, Phil. Trans. R. Soc. Lond. A **355** (1997) 2223.

[25] S. Chu, private communication.

[26] M. Kasevich, private communication.

[27] T. W. Darling, *et al.*, Rev. Mod. Phys. **64** (1992) 237.

[28] F. C. Witteborn and W. M. Fairbank, Phys. Rev. Lett. **19** (1967) 1049.

[29] See e.g. M. H. Holzscheiter, J. T. Goldman, and M. M. Nieto, in **New Frontiers in Hadronic Mechanics, Part III: Experimental and Theoretical Studies on Antimatter**, ed. T. L. Gili (Hadronic Press, 1996), p. 319.

[30] J. M. LoSecco, Phys. Rev. D **38** (1988) 3313.

[31] S. Pakvasa, W. A. Simmons, and T. J. Weiler, Phys. Rev. D **39** (1989) 1761.

[32] G. Gabrielse, Hyp. Int. **44** (1988) 349.

[33] N. Beverini *et al.*, Hyp. Int. **44** (1988) 357.

[34] R. Poggiani, Hyp. Int. **76** (1993) 371.

[35] J. Walz and T. W. Hansch, Gen. Rel. Grav. **36** (2004) 561.

[36] G. Drobychev *et al.*, "Proposal for the AEGIS experiment at the CERN Antiproton Decelerator," CERN-SPSC-2007-017, CERN-SPSC-P-334, June 2007, available from `http://doc.cern.ch//archive/electronic/cern/preprints/spsc/public/spsc-2007-017.pdf`

[37] P. Pérez *et al.*, "Letter of Intent to the CERN-SPSC: A new path to measure antimatter free fall," Nov. 29, 2007, available form `http://doc.cern.ch//archive/electronic/cern/preprints/spsc/public/spsc-2007-038.pdf`

[38] Draft minutes of the CERN SPSC January 2008 meeting, available from http://documents.cern.ch/cgi-bin/setlink?base=spsc&categ=public&id=spsc-2008-008

[39] http://www.hbartech.com